Volume 6 | Number 22 | 14 June 2018 | Pages 10153–10554

Journal of Materials Chemistry A

Materials for energy and sustainability

rsc.li/materials-a

ISSN 2050-7488

ROYAL SOCIETY OF CHEMISTRY

PAPER

Youju Huang, Tao Chen *et al.*

Designing a reductive hybrid membrane to selectively capture noble metallic ions during oil/water emulsion separation with further function enhancement

Journal of Materials Chemistry A

PAPER

View Article Online
View Journal | View Issue

Cite this: J. Mater. Chem. A, 2018, 6, 10217

Designing a reductive hybrid membrane to selectively capture noble metallic ions during oil/water emulsion separation with further function enhancement†

Lei Zhang,[a] Xianhu Zha,[b] Gui Zhang,[a] Jincui Gu,[a] Wei Zhang,[a] Youju Huang,*[a] Jiawei Zhang[a] and Tao Chen*[a]

Received 26th February 2018
Accepted 5th April 2018

DOI: 10.1039/c8ta01864b

rsc.li/materials-a

Owing to the ever-increasing demand for noble metals in modern industry, the extraction of noble metals from ores and electronic wastes is a significant topic. Conventional extraction means involving surfactants, organic solvents, and toxic extracting agents suffer from the limitation of complex heterogeneous separation and extraction operation as well as environmental pollution. Herein, a new carbon nanotube (CNT) hybrid membrane modified with eco-friendly and reductive poly acryloyl hydrazide (PAH) is reported, integrating the extraction of noble metal ions with heterogeneous emulsion separation. The hybrid membrane with underwater superoleophobic surface can achieve one-step preferential extraction of noble metal ions during oil/water emulsion separation, greatly simplifying the extraction operation. The reductive extraction yields nanoparticles loaded *in situ* on CNTs, which allows precise evaluation of the recovery performances by monitoring resistance variation of the hybrid membrane. Furthermore, the extracted hybrid membrane can be recycled for the catalytic conversion of organic contaminants as well as emulsion separation. The multi-functional hybrid membrane realizes comprehensive recovery of noble metal ions and heterogeneous separation for further recycling utilization, showing great potential for practical application towards the simple and integrated recycling of noble metals.

Introduction

The rapid development of modern industry, especially towards the information age, has put forward a huge demand for noble metal resources.[1–3] To realize the sustainable use of noble metal resources and reduce pollution, the extraction and recovery of noble metals from ores and electronic wastes are a significant topic.[4] On the basis of conventional recovery methods such as liquid–liquid extraction,[5] solid-phase extraction,[6] and precipitation,[7] many new attempts have been made based on new extracting agents to recover noble metals.[8,9] Generally, the present extraction of noble metal mainly includes pre-treatment and reductive extraction steps.[10] These operations usually require some surfactants and organic solvents for leaching, separation, and concentration of noble metal ions from solid ores and electronic waste.[11] The resultant heterogeneous organic/water mixture, even a surfactant-stabilized emulsion, cannot be used to directly extract noble metals ions or decrease the extraction efficiency for normal extracting materials due to surface pollution.[12] Some extra separation steps, such as demulsification or oil/water separation, are needed to recover noble metals and reduce pollution,[13] which inevitably lead to complex operation. If a robust extracting material integrates the oil/water separation function with the selective extraction of noble metals, it is expected to achieve direct extraction of noble metals from a heterogeneous organic/water mixture. This new eco-friendly extracting material will greatly simplify the operation and increase the recovery efficiency.

Inspired by the self-cleaning lotus leaf, superwettable membranes have drawn significant attention recently for the development of oil/water separation membranes.[14–16] For example, superhydrophobic and underwater superoleophobic carbon nanotube (CNT) membranes can effectively separate oil/water mixtures and even emulsions.[17–20] However, these normal superwettable membranes are limited by their inability to recover noble metal ions. Compared with other superwettable

[a]Key Laboratory of Marine Materials and Related Technologies, Zhejiang Key Laboratory of Marine Materials and Protective Technologies, Division of Polymers and Composite Materials, Ningbo Institute of Materials Technology and Engineering, Chinese Academy of Sciences, Ningbo 315201, China. E-mail: yjhuang@nimte.ac.cn; tao.chen@nimte.ac.cn

[b]Engineering Laboratory of Specialty Fibers and Nuclear Energy Materials, Ningbo Institute of Materials Engineering and Technology, Chinese Academy of Sciences, Ningbo, 315201, China

† Electronic supplementary information (ESI) available. See DOI: 10.1039/c8ta01864b

membranes, CNT membranes have inherent advantages as multi-functional membranes due to their flexible surface functionalization and porous network microstructures.[21–24] It is reasonably expected that appropriate absorbents, such as functional polymers containing specific ligands for noble metal ions,[4,25] integrate with the superhydrophilic/underwater superoleophobic CNT membrane to achieve direct recovery of noble metal ions during oil/water separation. Thus, it is desirable to design a unique separation membrane with flow-through manner of ion recovery and oil/water separation for simplifying the operation and for continuous industrial operation.[17] To efficiently recycle noble metal ions during oil/water separation, specific hydrophilic polymers with strong and selective reducibility towards noble metal ions are crucial. Hydrazide derivatives, well-known ligands for metal ions and some organic molecules,[26] had been seldom reported for the selective reducibility of noble metal ions. Recently, a hydrogel containing hydrazide groups has shown rapid and selective reducing capacity for noble metal ions in an aqueous solution;[27] this indicates that the integration of a hydrazide-containing polymer material with the superwettable carbon nanotube membrane has great potential for achieving direct recovery of noble metal ions during the oil/water separation process.

In the present study, CNTs modified with reductive polyacryloyl hydrazide (PAH) brushes assembled into a superhydrophilic/underwater superoleophobic hybrid membrane, integrating heterogeneous emulsion separation with the extraction of noble metal ions. The resultant hybrid membrane can achieve one-step selective extraction of noble metal ions during oil/water emulsion separation, which greatly simplifies the extraction operation (Scheme 1A). Moreover, the reductive extraction of noble metal ions yields nanoparticles (NPs) *in situ* loaded on CNTs (Scheme 1B) and gradually decreases the resistance of the hybrid membrane, which allows timely control or precise evaluation of recovery performances by monitoring the resistance variation of the hybrid membrane. Furthermore, the hybrid membrane containing recovered noble metal nanoparticles can be recycled for the catalytic decomposition of organic contaminants and simultaneous separation of oil/water emulsions, achieving the recycling utilization of waste noble metal ions (Scheme 1C). Unlike conventional separation membranes, this novel multi-functional hybrid membrane realizes comprehensively one-step recovery of noble metal ions and heterogeneous separation as well as recycling utilization. This indicates that this hybrid membrane has great potential for practical application in the simple and integrated recycling of noble metals.

Experimental

Materials

Multi-walled carbon nanotubes (diameter, about 10–30 nm; length, about 10–30 μm; –COOH wt%, about 1.5%) were

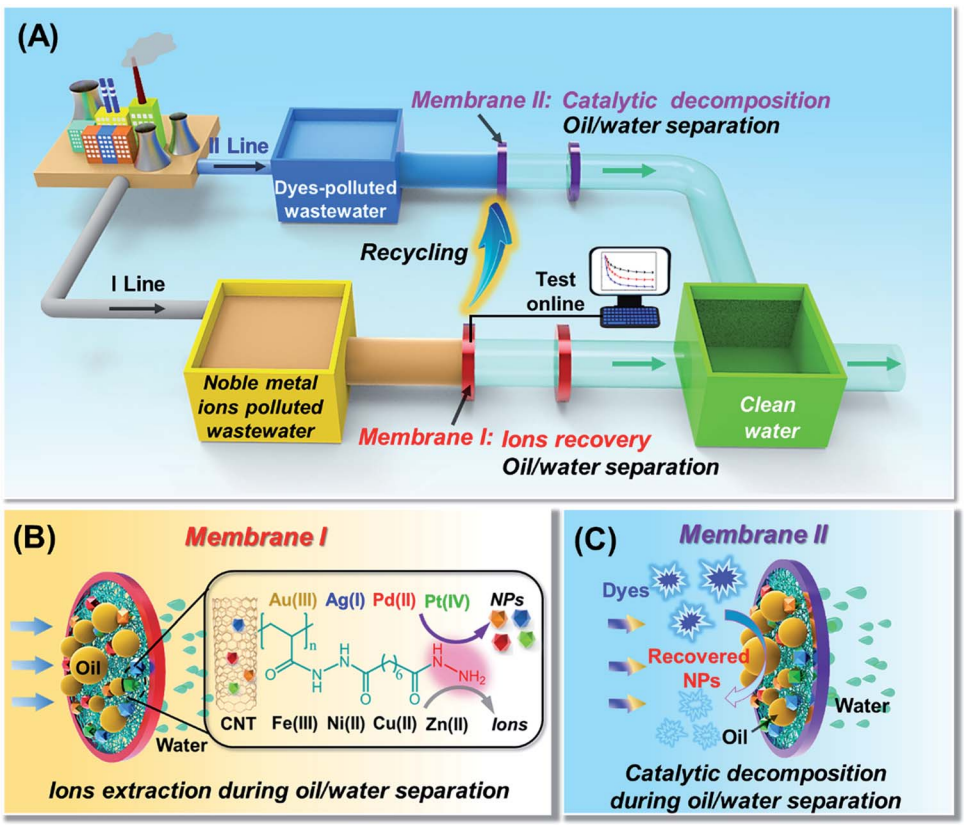

Scheme 1 Schematic of the selective recovery of noble metal ions during oil/water separation (A and B) and the recycling utilization during the catalytic decomposition of dyes in oily wastewater using the CNT/PAH composite separation membrane (C).

purchased from Chengdu Organic Chemistry Co., Ltd. Acrylic acid (AA), 2,2-azobisisobutyronitrile (AIBN), and silver nitrate ($AgNO_3$, 99%) were provided by Sinopharm Chemical Reagent Co., Ltd in Shanghai. Acrylic acid was refined by vacuum distillation. AIBN was recrystallized thrice in methanol before use. Adipic dihydrazide (99%) and *N*,*N*′-carbonyldiimidazole (99%) were purchased from Aladdin Industrial Corporation (Shanghai). Chloroauric acid ($HAuCl_4 \cdot 4H_2O$, 99.9%), chloroplatinic acid ($H_2PtCl_6 \cdot 6H_2O$, 99.9%), and palladium chloride ($PdCl_2$, 99.9%) were purchased from Sigma-Aldrich. The hydrophilic polyvinylidene fluoride (PVDF) micro-filtration membrane (aperture size, 0.45 μm) was obtained from Merck Milipore Ltd. (Ireland). Other chemicals including organic solvents and the surfactant Tween-80 were purchased from Sinopharm Chemical Reagent Co., Ltd (Shanghai) and used as received. Milli-Q-grade water (18.2 MΩ cm) was used in all the experiments.

Preparation of the polyacryloyl hydrazide-modified CNT composite (CNT/PAH)

Typically, 0.1 g of CNTs was dispersed in 100 mL of acetone by sonication, and then, 1.0 g of acrylic acid was added to the CNT dispersion. After being bubbled with dry nitrogen for 30 min, 55 mg of AIBN was added to the mixture and stirred for 8 h in an oil bath at 55 °C. The resultant CNT/PAA hybrid was refined by three cycles of filtration, redispersion, and washing with ethanol before being dried for 24 h at 45 °C. Subsequently, 0.1 g of CNT/PAA was dispersed uniformly in 50 mL dimethylformamide (DMF). *N*,*N*′-Carbonyldiimidazole solution in DMF (10 mL, 0.1 g mL^{-1}) was added to the abovementioned CNT/PAA dispersion and stirred overnight at room temperature. The resultant mixture was added dropwise to the adipic dihydrazide solution (10 g, 50 mL DMF) and stirred for 24 h at 45 °C. Upon reaction completion, the raw product CNT/PAH was obtained by vacuum filtration and refined by washing with ethanol before being dried for 24 h at 30 °C.

Preparation of the CNT/PAH hybrid membranes

CNT/PAH (5 mg) was dispersed in 50 mL H_2O by sonication and then poured onto a PVDF membrane held in a vacuum filtration setup. After filtration under vacuum at 0.1 MPa, a smooth composite membrane was formed supported on the PVDF membrane.

Characterization

The microstructures of CNTs and composite membrane were characterized mainly by scanning electron microscopy (JEOL JSM-6700F scanning electron microscope) and transmission electron microscopy (JEOL JEM 2010 electron microscope). The composition of CNT/PAH was analyzed by Fourier transform infrared spectroscopy (FTIR) and X-ray photoelectron spectroscopy (XPS). FTIR spectroscopy was conducted using Thermo Nicolet 6700 FT-IR spectrometer, whereas XPS analysis was performed *via* a Shimadzu Axis Ultra DLD spectroscope with MgK_α as the radiation source. The weight ratio of PAH on CNTs was measured using a Netzsch TG 209F1 instrument at the heating rate of 10 °C min^{-1} under a N_2 atmosphere. The extraction content of the recovered noble metal nanoparticles was tested by inductively coupled plasma-atomic emission spectrometry (ICP-MS, Optima 2100, Perkin-Elmer). UV/vis absorption measurement was conducted using a LAMBDA 950 UV-vis spectrometer. Static water and oil contact angles in air or under water were determined using OCA-20 Data Physics instruments at room temperature; 3 μL of liquid droplet was dropped on the membrane, and an average of three measurements was made to determine the surface wettability. The emulsion and filtrate solution were analyzed by BX 51TF Instec H601. Dynamic light scattering (DLS) measurements were performed using a Zetasizer Nano ZS. The resistance of the hybrid membrane was tested using a Keysight 34461A digital multimeter. Before the resistance measurement, the hybrid membrane was refreshed by washing with water and ethanol at least twice and then dried with blowing air (35 °C) for 5 min.

Results and discussion

The strategy developed for fabricating the multi-functional hybrid membrane is schematically illustrated in Fig. 1A. Hydrophilic polyacrylic acid (PAA) brushes were covalently grafted on CNTs by radical polymerization. After further reaction with adipic dihydrazide (ADH), polyacryloyl hydrazide (PAH)-modified CNTs were constructed. Subsequently, the prepared CNT/PAH assembled into a close-packed hybrid membrane by vacuum filtration on the supported PVDF membrane (Fig. 1A). The microstructures and composition of CNT/PAH were characterized in detail, and the results are shown in Fig. S1.† The SEM image shows that the surface of CNTs is coated with a hydrophilic polymer shell, which endows CNTs with good dispersion in water (Fig. S1A†). In the FTIR spectrum, a vibration peak of the carboxyl group is shown at 1724 cm^{-1}, and a strong stretching peak around 3500 cm^{-1} is attributed to the NH_2 group from hydrazide (Fig. S1B†).[28,29] In the XPS spectrum, the CNT hybrid exhibits three typical peaks of C 1s, O 1s, and N 1s (Fig. S1C†). The high resolution spectrum of C 1s shows four typical split peaks at 284.60, 285.45, 286.65, and 289.25 eV,[30] assigned to sp^2 C=C, sp^3 C–C, C–O, and COO energy bonds, respectively (Fig. S1D†). Moreover, the high resolution spectrum of N 1s exhibits C–N and –NH energy bands at 4002.2 and 401.6 eV, respectively (Fig. S1E†).[31] These FTIR and XPS results indicate the successful functionalization of PAH on CNTs. The weight ratio of PAH in the hybrid was characterized by TGA analysis (Fig. S1F†). The weight loss in the range 50–400 °C indicates that the weight proportion of PAH is about 18%.[32]

Upon vacuum filtration, CNT/PAH assemble into a smooth membrane (Fig. 1A).[17] The obtained hybrid membrane has good wettability towards both toluene and water in air, whereas it shows distinct superoleophobic behaviour in water (Fig. 1B, Movie S1†). Except for toluene, the hybrid membrane shows similar wettability for other organic solvents such as dichloromethane, hexane, and chloroform (Fig. 1C). The contact angles (CAs) of water and organic solvents on the membrane are used to evaluate the surface wettabilities in air and water. The CAs of

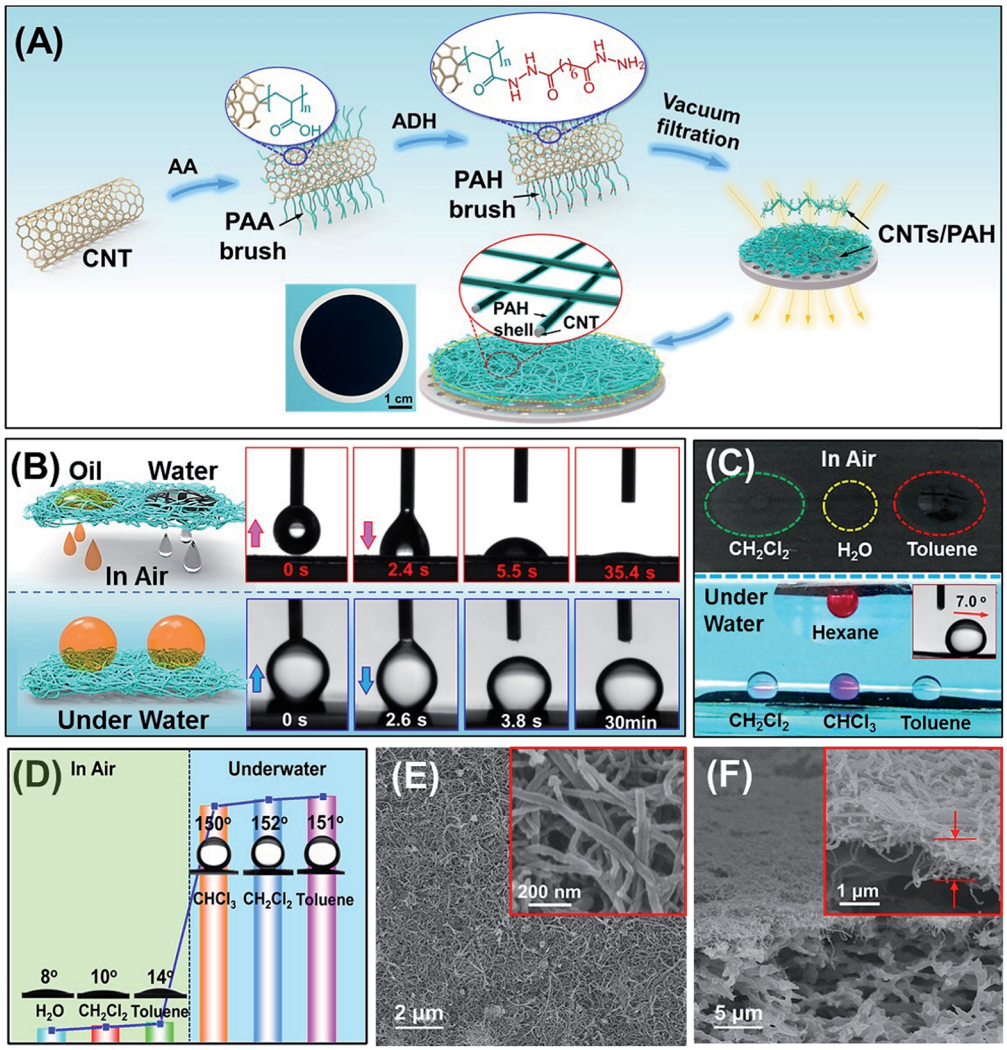

Fig. 1 (A) Schematic of fabrication of CNT/PAH hybrid membrane. (B) Surface wettabilities of the membrane for dichloromethane (B) and other solvents (C) in air and in water. The organic solvents are dyed with different colours. The inset shows the rolling angle of the dichloromethane drops on the membrane. (D) Contact angles of solvents on the membrane in air and in water. (E and F) SEM images of the surface and cross-section of the hybrid membrane.

both water and organic solvents, such as toluene and dichloromethane, are below 14° in air, whereas the underwater CA of organic solvents exceeds 150°, showing superhydrophilic/superoleophilic features in air and superoleophobic feature under water (Fig. 1D).[33,34] Further observation by SEM of the microstructure of the hybrid membrane indicates that CNTs overlap compactly with each other and assemble into a porous network membrane with a uniform thickness of about 1 μm. These porous microstructures and nanoscale rough surfaces, integrating with hydrophilic PAH brush shells, are considered to be responsible for the underwater superoleophobic wettability.[35] The porosity of the membrane is determined to be about 105 nm, showing the capability of the membrane to act as an ultrafiltration membrane.[36] The nanoscale porous structures and underwater superoleophobic surface allow this hybrid membrane to selectively remove oil from water.

To evaluate the oil/water separation performance, an oil-in-water emulsion of toluene/water (v/v, 3.3%) stabilized by Tween 80 was selected as a model. The emulsion was added directly to the common filtration separation setup installed with the CNT/PAH hybrid membrane (Fig. S2A†). After suction filtration at a pressure of 0.1 MPa, the oil droplets in the filtrate solution and feed emulsion were characterized by optical microscopy and diameter analysis to examine the oil/water separation efficiency (Fig. S2B and C†). It was found that the filtrate solution hardly contained micron-sized oil droplets except nanoscale oil droplets with an average size of 30 nm (Fig. S2D and E†). The results indicate that this hybrid membrane has high retention ability for oil droplets above 30 nm. The fluxes of various emulsions passing through the membranes were also measured, and similar separation fluxes were obtained (Fig. S2F†). Upon ten recycles of separation, the flux reduced slightly and remained around 3500 L

m^{-2} h^{-1} bar $^{-1}$ (Fig. S2G†), showing good stability and reproducibility.

Hydrophilic PAH brushes also show reduction ability for noble metal ions, which allow the CNT/PAH hybrid membrane to simultaneously extract noble metal ions during oil/water separation. To investigate the recovery performance of the hybrid membrane for noble metal ions, extraction of Au(III) ions was selected as a model process. The chloroauric acid ($HAuCl_4$) aqueous solution, used as a Au ion source, was mixed with toluene to form a model emulsion (v/v, 3.3%) with the assistance of the surfactant Tween 80. To timely detect the recovery process, the CNT/PAH hybrid membrane was fixed with a copper foil electrode to show the resistance changes of the hybrid membrane during extraction. Clamped with two PDMS spacers, the membrane was immobilized between the junctions of two tubes, as shown in Fig. 2A.

The emulsion containing Au ions (0.1 mM [$AuCl_4^-$]) was added to the feed tank, and the filtrate receiver tank was connected to a vacuum pump to drive the emulsion through the hybrid membrane under a low pressure of 0.01–0.02 MPa (Fig. 2B). After filtration at a stable flux of 250 L m^{-2} h^{-1}, the heterogeneous emulsion changed distinctly to a clear aqueous solution (Fig. 2B, Movie S2†). The oil droplets in the feed and filtrate were characterized by optical microscopy and dynamic light scattering. It was found that a large amount of micron-sized oil droplets in feed solution were removed clearly, and only nanoscale oil droplets below 30 nm remained in the filtrate (Fig. 2C–E). To further test precisely the content of toluene in the filtrate, the relationship between characteristic absorption intensity of toluene and content was obtained and fitted linearly (Fig. S3†). The content of toluene in the filtrate solution was about 0.39 mg L^{-1}, and 98.6% of toluene was removed; this indicated high emulsion separation ability. After oil/water

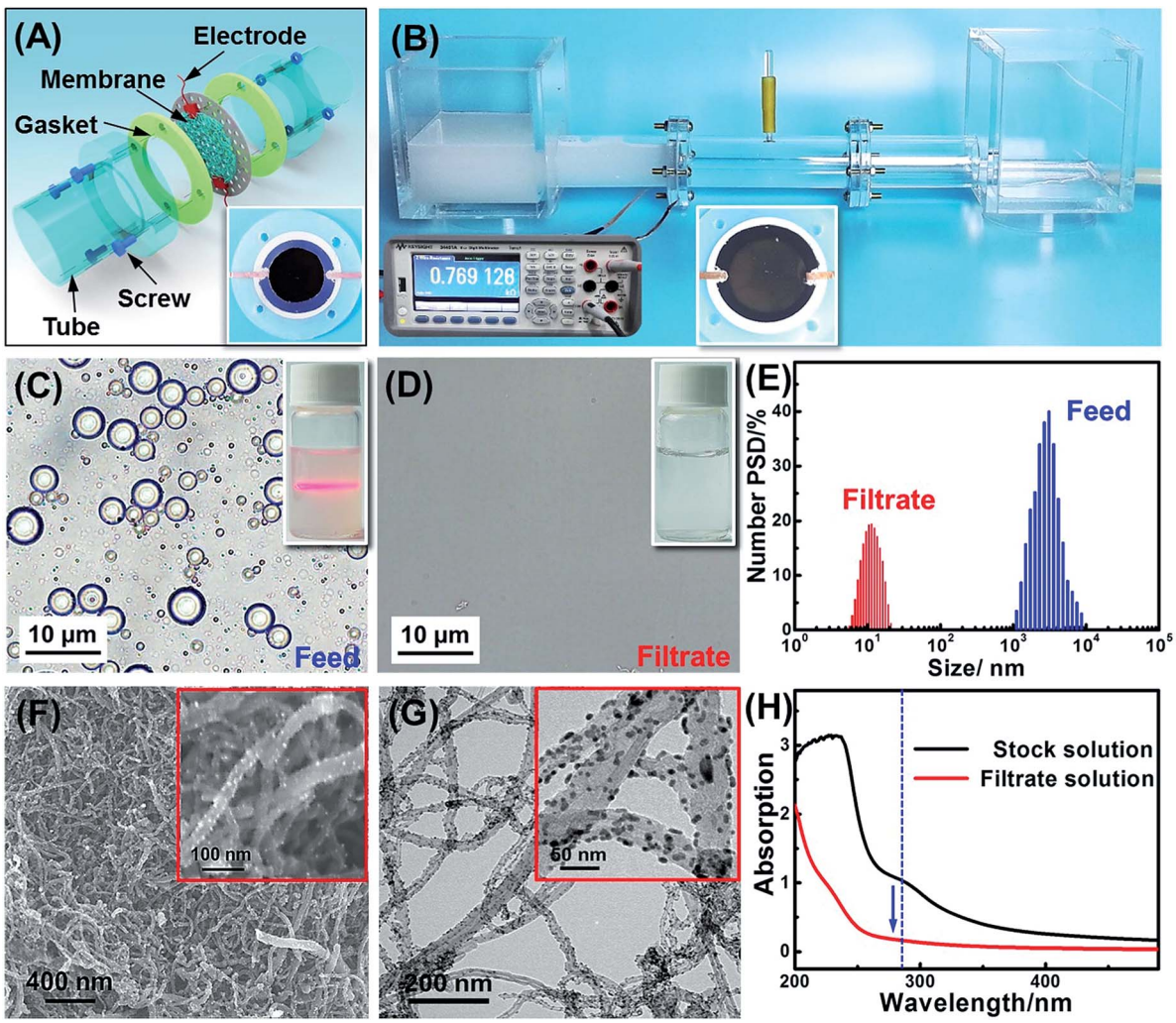

Fig. 2 (A) Schematic of the hybrid membrane hold in the conjugation between two tubes. The inset shows the hybrid membrane fixed with an electrode. (B) An image of toluene/water emulsion separation and extraction of Au ions. The inset shows the resistance of the membrane and its surface after extraction. (C and D) Optical image of feed emulsion and filtrate. The inset show the images of feed emulsion and filtrate solution, respectively. (E) Size distribution of oil droplets in feed emulsion and filtrate. SEM image (F) and TEM image (G) of the hybrid membrane after extracting AuNPs. (H) UV/vis absorption of $AuCl_4^-$ ions in the feed emulsion and filtrate solution.

separation, the surface of the hybrid membrane still remained clean and showed a brownish red or yellow colour (the inset in Fig. 2B), implying the existence of Au NPs in the membrane. The microstructure of the hybrid membrane was observed by electron microscopy and further characterized by energy dispersive spectroscopy. SEM and TEM images show that large amounts of small-sized Au NPs are absorbed on the surface of CNTs (Fig. 2F, G, and S4A†). Au ions are reduced to nanoparticles by PAH and anchor *in situ* on CNTs during oil/water separation. The concentration variation of $AuCl_4^-$ ions before and after recovery was tested based on the absorption intensity (Fig. 2H). When 10 mL of emulsion with 0.1 mM [$AuCl_4^-$] passed through the composite membrane, the concentration of $AuCl_4^-$ ions in the filtrate solution decreased to about 6.5×10^{-3} mM, and the yield was about 93% during oil/water separation.

The attachment of Au NPs on CNTs can reduce the resistance of the hybrid membrane. Thus, the resistance change of the hybrid membrane can be used to evaluate the ion extraction process and exactly evaluate the recovery performance.[37,38] During oil/water separation, the flux was set at a constant value of 250 L m^{-2} h^{-1}, and the resistance of the hybrid membrane was obtained continuously in response to the separation time and [$AuCl_4^-$] value in the emulsion (Fig. 3A). The original resistance of the hybrid membrane was about 0.93 kΩ ± 0.02 kΩ keeping the amount of CNT/PAH hybrid constant at 4 mg ± 0.2 mg (the area of the membrane was about 13.8 cm^2). In the initial stage, the resistance of the hybrid membrane reduced rapidly in a short time and then tended to an equilibrated value after about 100 min. This indicated the rapid recovery ability of the PAH shells toward $AuCl_4^-$ ions. The final resistance of the membrane decreased gradually when [$AuCl_4^-$] varied from 0.001 mM to 0.5 mM. To precisely investigate the resistance changes in the recovery process, the resistance was plotted and fitted nonlinearly in response to the extraction time and [$AuCl_4^-$]. The resistance changes ($\Delta R = R' - R_0$) have been discussed quantitatively based on the fitted curves shown in Fig. 3A, where R_0 is the original resistance of the hybrid membrane and R' represents the resistance at time t. The variation $\Delta R_t/\Delta R_{max}$ in response to time and [$AuCl_4^-$] was calculated, where ΔR_t is ΔR at time t and ΔR_{max} is the maximum value of ΔR. The time required for change of $\Delta R_t/\Delta R_{max}$ from 5% to 50% ($t_{50} - t_5$) and from 5% to 90% ($t_{90} - t_5$) in response to [$AuCl_4^-$] is shown in Fig. 3B. It is found that the time required for both stages of ($t_{50} - t_5$) (rhombus) and ($t_{90} - t_5$) (circle) decreases with the increasing [$AuCl_4^-$], but their variation tendencies are distinctly different. The time needed in the stage ($t_{50} - t_5$) decreases nonlinearly and changes rapidly below 0.2 mM [$AuCl_4^-$] until slowly approaching an equilibrated state above 0.5 mM. However, in the entire variation of the ($t_{90} - t_5$) stage, the required time decreases linearly with the increasing [$AuCl_4^-$]. Furthermore, the slope of the $\Delta R_t/\Delta R_{max}$ fitted curve at $\Delta R_t/\Delta R_{max}$ = 50% (S_{50}) increases exponentially with the increasing [$AuCl_4^-$] (Fig. 3C). This indicates a faster dynamic reducing rate at higher [$AuCl_4^-$]. These results of the resistance changes indicate that the overall recovery process during oil/water separation is considered to be mainly dependent on [$AuCl_4^-$] although [$AuCl_4^-$] also dramatically affects the kinetic process.

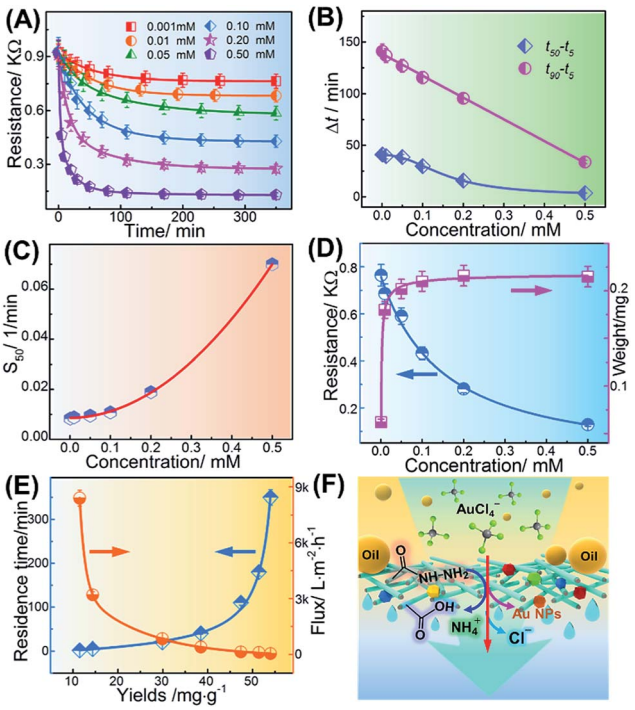

Fig. 3 (A) Time-dependent resistance variation of the hybrid membrane in response to different [$AuCl_4^-$] during emulsion separation. [$AuCl_4^-$] was 0.001, 0.01, 0.05, 0.1, 0.2, or 0.5 mM. (B) Effects of [$AuCl_4^-$] on the time required for changes of $\Delta R_t/\Delta R_{max}$ from 5% to 50% ($t_{50} - t_5$) (rhombus) and from 5% to 90% ($t_{90} - t_5$) (circle). (C) Effects of [$AuCl_4^-$] value on the slope (S_{50}) of $\Delta R_t/\Delta R_{max}$ curves at $\Delta R_t/\Delta R_{max}$ = 50%. (D) The plotted curves of final resistance and maximum recovered content in response to [$AuCl_4^-$]. (E) The plotted curves of recovered yield against residence time and separation flux. (F) Schematic of the extraction mechanism of Au ions during oil/water separation.

To accurately evaluate the effects of [$AuCl_4^-$] on the recovery results, the relationship between resistance and [$AuCl_4^-$] value in the range 0.001–0.5 mM is achieved based on the terminal resistance value, as shown in Fig. 3A. The results are shown in Fig. 3D (circles), and the corresponding fitted curves can be expressed as $R = 11.34\,[AuCl_4^-]^2 + 8.32\,[AuCl_4^-] + 1.32$ (R-square = 0.995). Additionally, to verify effectiveness based on resistance evaluation, the extracted amount of Au NPs in the membrane was detected directly by testing the mass of NPs. The recovered Au NPs on the membrane were dissolved in chloroauric acid, and the content of Au NPs was characterized quantitatively using ICP-MS (Fig. 3D, cube). Upon sufficient recovery (3 h), the content of the extracted AuNPs increases rapidly with the increasing [$AuCl_4^-$] until approaching the maximum above 0.2 mM [$AuCl_4^-$]. It is determined that about 0.21 mg of AuNPs are extracted in the hybrid membrane. Based on the TGA result of CNT/PAH (PAH, 18 wt%), the content of PAH in the hybrid membrane (gross weight: 4 mg) was about 0.72 mg. Thus, the maximum uptake capacity of the membrane for Au ions is estimated to be as high as 292 mg g^{-1} (metal/PAH).

During the dynamic separation and recovery process, the flux and residence time of the emulsion are also important influencing factors. The maximum recovery yields of the hybrid membrane against flux or residence time are plotted (Fig. 3E). In each cycle of recovery, 300 mL emulsion containing 0.1 mM [$AuCl_4^-$] was treated at different fluxes, and the corresponding residence time could be calculated. When the flux is below 840 L m^{-2} h^{-1} or the residence time exceeds 50 min, the content of the extracted AuNPs exhibits relatively higher yields in the range 175–246 mg g^{-1} (metal/PAH). With the increasing flux, the yield decreases dramatically below 60 mg g^{-1}. Sufficient exposure of ions to reductive PAH coating allows more ions to be reduced to nanoparticles. The reducibility of PAH is ascribed to the hydrazide group –CO–NH–NH_2.[39,40] During the reductive reaction between the hydrazide group and noble metal ions, hydrazide groups are oxidized to ammonium ions, whereas the metal ions are reduced to atoms, which gradually grow into NPs and anchor *in situ* on CNTs (Fig. 3F).

More interestingly, this PAH-modified hybrid membrane exhibits good selectivity for noble metal ions and can selectively extract silver (Ag), palladium (Pd), and platinum (Pt) ions in addition to Au ions (Fig. 4). There were large-sized nanoparticles or aggregates absorbed on the membrane extracting Ag and Pd ions (Fig. 4A and B), whereas small-sized Pt NPs were obtained on the membrane extracting Pt (Fig. 4C). These differently shaped noble metal nanoparticles are attributed to the different reduction rates arising from their reduction potentials.[27] On the other hand, these was hardly any nanoparticle produced on the membrane when it was treated with an emulsion containing common metal ion mixtures such as Cu^{2+}, Ni^{2+}, Fe^{3+}, and Zn^{2+} (Fig. 4D). These results show the selective extraction behaviour of the membrane towards noble metal ions. To understand the selectivity mechanism of PAH for noble metal ion recovery, the thermodynamics and kinetic reaction process between PAH and metal ions were simulated based on first-principles. According to previous studies,[39,40] the reductive hydrazide group –CO–NH–NH_2 in PAH is inferred to be protonated in water and forms the more active intermediate (NH_2–NH_3^+) after the electron transfer steps. Subsequently, the intermediate NH_2–NH_3^+ is oxidized by metal ions to ammonium salt. Moreover, the carbonyl group finally transforms into the carboxylate group. The possible chemical reactions between hydrazide and metal ions are proposed and presented in Fig. S5.†

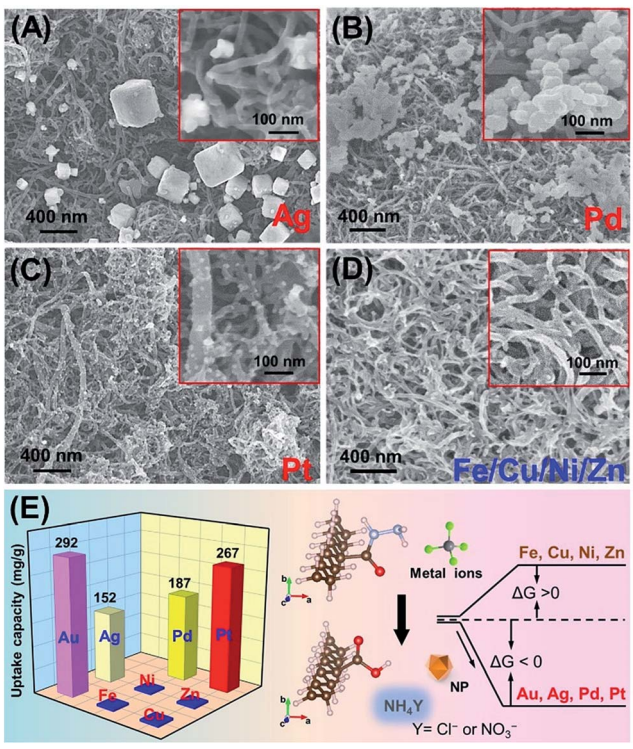

Fig. 4 SEM images of the hybrid membranes after extracting Ag (A), Pd (B), Pt (C), and mixed Fe/Cu/Ni/Zn ions (D). (E) The uptake capacity of hybrid membrane for metal ions (left) and Gibbs energy changes in the reductive reaction involving PAH and metal ions (right).

As is well-known, Gibbs energy is a crucial factor that demonstrates whether a chemical reaction can spontaneously occur,[41,42] and thus, it is calculated herein based on the first-principles simulation (Fig. S6†). Since entropy and pressure generally show negligible influences on the magnitude of Gibbs energy,[43] these contributions are excluded. Herein, the main chain structure of PAH is simulated simplistically using $C_{10}H_{19}$ with one branched hydrazide group (Fig. 4E). Thus, the interactions between branched structures could be ignored based on the large lattice parameter in the periodic *c*-axis approximated as 12.8 Å. The metal complexes were studied with cluster models. The optimized structures of reactants and carboxylate product of PAH are provided in Fig. S6,† except for the water molecule. According to the optimized structures and the proposed possible reactions, the Gibbs energy of each chemical equation is calculated and provided in Table S1.† Compared with that of common metal ions, negative Gibbs energies between noble metal ions and hydrazide group indicate that these reactions can occur spontaneously (Fig. 4E), which can be responsible thermodynamically for the selective extraction of noble metal ions by the PAH-modified hybrid membrane.

The recovered noble nanoparticles endow the hybrid membrane with significant catalytic activity,[44] which can be recycled for the catalytic conversion of organic contaminants in water. These extracted hybrid membranes, possessing stable superoleophobic surfaces and recovered noble metal NPs, are capable of treating oily wastewater containing organic pollutants. Hybrid membranes loaded with recycled Au or Pd NPs are selected representatively to investigate their recycling application in the treatment of organic polluted wastewater. To test the catalytic performance of the recovered AuNPs, the well-known reduction reaction in which yellow 4-nitrophenol (4-NP) is converted into colorless 4-aminophenol using $NaBH_4$ as the reductive agent is employed as a model. When the toluene/water emulsion containing 25 mM 4-nitrophenol (0.25 M $NaBH_4$) is poured into the separation setup, the colorless aqueous solution flows out (Fig. 5A, Movie S3†); this indicates the effective catalytic ability of the recovered AuNPs as well as the oil/water separation performance. The distinctive color change is attributed to the catalytic conversion of the NO_2 group

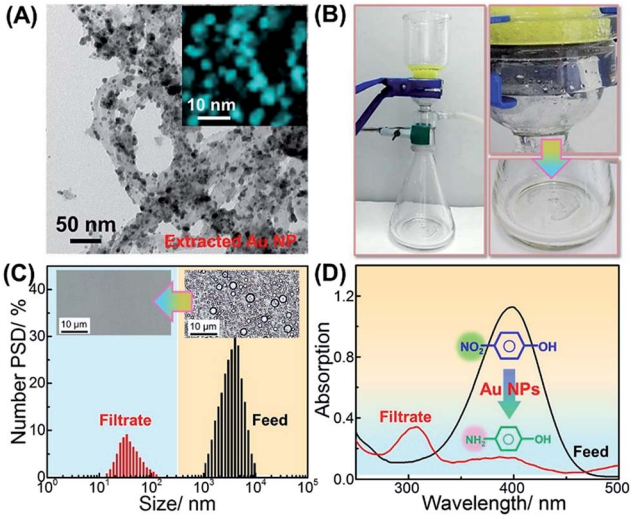

Fig. 5 Recycling utilization of the hybrid membrane containing extracted Au NPs. (A) An image of the catalytic decomposition of 4-nitrotoluene during oil/water separation (B). Size distributions of oil droplets in feed emulsion and filtrate solution (C). The inset shows optical images of the feed emulsion and filtrate solution (D) UV/vis absorption spectra of 4-nitrotoluene before and after separation.

to the NH_2 group in the presence of $NaBH_4$. In addition, an emulsion containing methylene blue was used to verify the catalytic performance of the extracted Pd during oil/water separation (Fig. S7†). Toluene/water emulsion containing MB (37.5 mM, 2.6 M $NaBH_4$) was purified directly into a homogenous colourless aqueous solution upon passing it through the membrane loaded with Pd NPs (Movie S4†). Moreover, these recycled composite membranes can be repeatedly used to catalytically purify organic polluted emulsions without obvious efficiency reduction with limited repetitions (Fig. S8A and B†). After 18 cycles of recycling separation, the partial composite membrane containing Pd NPs was observed by TEM (Fig. S8C†). It is not obvious that nanoparticles fall off the membrane. It is considered that these extracted nanoparticles attached on the CNTs do not cause remarkable secondary pollution under limited cycles of recycling. The oil/water separation and catalytic performances completely indicate that the CNT/PAH hybrid membrane not only extracts noble metal ions directly from heterogeneous oil/water mixtures, but also achieves further recycling utilization of the recovered noble metal NPs such as in wastewater purification.

Conclusions

In summary, we demonstrated a multi-functional CNT/PAH hybrid membrane with selective recovery of noble metal ions during oil/water emulsion separation. This CNT hybrid membrane containing recovered nanoparticles can be recycled for further application in water purification such as in the catalytic decomposition of organic contaminants and oil/water separation. The extraction of $AuCl_4^-$ ions by the hybrid membrane was evaluated precisely by monitoring the resistance variation. It was found that the overall recovery process during oil/water separation depended mainly on [$AuCl_4^-$] and related kinetics processes. The maximum uptake capacity of the hybrid membrane is estimated to be about 292, 152, 187, and 267 mg g^{-1} (metal: PAH) for Au, Ag, Pd, and Pt ions, respectively. These hybrid membranes, acting as a simple, eco-friendly extraction materials, can realize comprehensively one-step recovery of noble metal ions and heterogeneous separation for further recycling utilization, which are significant for the sustainable development of modern industry relying on noble metal resources.

Conflicts of interest

There are no conflicts to declare.

Acknowledgements

We thank the Natural Science Foundation of China (51603219, 51473179, 11604346, 51603216), Ningbo Science and Technology Bureau (2017D10001, 2015C110031), Open Research Fund of Key Laboratory of Marine Materials and Related Technologies (2016Z01, 2017K03), Bureau of Frontier Science and Education of Chinese Academy of Sciences (QYZDB-SSW-SLH036), and Youth Innovation Promotion Association of Chinese Academy of Sciences (2016268, 2017337).

References

1 Z. Fan and H. Zhang, *Chem. Soc. Rev.*, 2016, **45**, 63–82.
2 M. J. Sailor and J. H. Park, *Adv. Mater.*, 2012, **24**, 3779–3802.
3 Y. J. Liu, Z. T. Wang, Y. Liu, G. Z. Zhu, O. Jacobson, X. Fu, R. L. Bai, X. Y. Lin, N. Lu, X. Y. Yang, W. P. Fan, J. B. Song, Z. Wang, G. C. Yu, F. W. Zhang, H. Kalish, G. Niu, Z. H. Nie and X. Y. Chen, *ACS Nano*, 2017, **11**, 10539–10548.
4 P. Yang, C. Yue, H. Sun, W.-J. Liu, X. Deng, B. G. Guan and X. Zhang, *Angew. Chem., Int. Ed.*, 2017, **56**, 9331–9335.
5 R. S. Marinho, J. C. Afonso and J. da Cunha, *J. Hazard. Mater.*, 2010, **179**, 488–494.
6 N. Jalilian, H. Ebrahimzadeh, A. A. Asgharinezhad and K. Molaei, *Microchim. Acta*, 2017, **184**, 2191–2200.
7 O. D. Sant'Ana, A. L. R. Wagener, R. E. Santelli, R. J. Cassella, M. Gallego and M. Valcarcel, *Talanta*, 2002, **56**, 673–680.
8 M. Gurung, B. B. Adhikari, S. Morisada, H. Kawakita, K. Ohto, K. Inoue and S. Alam, *Bioresour. Technol.*, 2013, **129**, 108–117.
9 M. Gras, N. Papaiconomou, N. Schaeffer, E. Chainet, F. Tedjar, J. A. P. Coutinho and I. Billard, *Angew. Chem., Int. Ed.*, 2018, **130**, 1579–1582.
10 E. Mladenova, I. Karadjova and D. L. Tsalev, *J. Sep. Sci.*, 2012, **35**, 1249–1265.
11 J. Ponou, L. P. Wang, G. Dodbiba and T. Fujita, *Sep. Purif. Technol.*, 2018, **191**, 86–93.
12 A. Shah, S. Shahzad, A. Munir, M. N. Nadagouda, G. S. Khan, D. F. Shams, D. D. Dionysiou and U. A. Rana, *Chem. Rev.*, 2016, **116**, 6042–6074.

13 L. N. Andrade, C. C. Amorim, S. V. Santos, I. F. Teixeira, M. M. D. Leão and R. M. Lago, *Chem. Eng. J.*, 2015, **271**, 281–286.
14 L. P. Wen, Y. Tian and L. Jiang, *Angew. Chem., Int. Ed.*, 2015, **54**, 3387–3399.
15 Z. L. Chu, Y. J. Feng and S. Seeger, *Angew. Chem., Int. Ed.*, 2015, **54**, 2328–2338.
16 H. C. Yang, J. Hou, V. Chen and Z. K. Xu, *Angew. Chem., Int. Ed.*, 2016, **55**, 13398–13407.
17 L. Zhang, J. C. Gu, L. P. Song, L. Chen, Y. J. Huang, J. W. Zhang and T. Chen, *J. Mater. Chem. A*, 2016, **4**, 10810–10815.
18 J. C. Gu, P. Xiao, J. Chen, J. W. Zhang, Y. J. Huang and T. Chen, *ACS Appl. Mater. Interfaces*, 2014, **6**, 16204–16209.
19 J. C. Gu, P. Xiao, J. Chen, F. Liu, Y. J. Huang, G. Y. Li, J. W. Zhang and T. Chen, *J. Mater. Chem. A*, 2014, **2**, 15268–15272.
20 J. C. Gu, P. Xiao, Y. J. Huang, J. W. Zhang and T. Chen, *J. Mater. Chem. A*, 2015, **3**, 4124–4128.
21 S. J. Gao, Z. Shi, W. B. Zhang, F. Zhang and J. Lin, *ACS Nano*, 2014, **8**, 6344–6352.
22 Z. Shi, W. B. Zhang, F. Zhang, X. Liu, D. Wang, J. Jin and L. Jiang, *Adv. Mater.*, 2013, **25**, 2422–2427.
23 L. Hu, S. J. Gao, X. G. Ding, D. Wang, J. Jiang, J. Jin and L. Jiang, *ACS Nano*, 2015, **9**, 4835–4842.
24 A. Asthana, T. Maitra, R. Buchel, M. K. Tiwari and D. Poulikakos, *ACS Appl. Mater. Interfaces*, 2014, **6**, 8859–8867.
25 D. M. Han, Q. M. Zhang and M. J. Serpe, *Nanoscale*, 2015, **7**, 2784–2789.
26 D. W. Zhang, X. Zhao and Z. T. Li, *Acc. Chem. Res.*, 2014, **47**, 1961–1970.
27 B. O. Okesola, S. K. Suravaram, A. Parkin and D. K. Smith, *Angew. Chem., Int. Ed.*, 2016, **55**, 183–187.
28 S. J. Byard, M. Williams, B. E. McKenzie, A. Blanazs and S. P. Armes, *Macromolecules*, 2017, **50**, 1482–1493.
29 P. Zabierowski, M. Oszajca, M. Hodorowicz and D. Matoga, *Polyhedron*, 2017, **121**, 25–32.
30 M. G. Neira-Velázquez, E. Hernández-Hernández, L. F. Ramos-deValle, C. A. Ávila-Orta, Y. A. Perera-Mercado, S. G. Solís-Rosales, P. González-Morones, A. Ponce-Pedraza, M. Ávalos-Borja, R. I. Narro-Céspedes and P. Bartolo-Pérez, *Plasma Processes Polym.*, 2013, **10**, 627–633.
31 S. Y. Xiao, Q. Z. Xiong, H. J. Zhou, Y. X. Zhang, G. Z. Wang, H. M. Zhang and H. J. Zhao, *J. Appl. Polym. Sci.*, 2016, **133**, 8.
32 C. Kaewtong, S. Kampaengsri, B. Singhana and B. Pulpoka, *Dyes Pigm.*, 2017, **141**, 277–285.
33 F. Zhang, W. B. Zhang, Z. Shi, D. Wang, J. Jin and L. Jiang, *Adv. Mater.*, 2013, **25**, 4192–4198.
34 P. C. Chen and Z. K. Xu, *Sci. Rep.*, 2013, **3**, 6.
35 B. W. Xin and J. C. Hao, *Chem. Soc. Rev.*, 2010, **39**, 769–782.
36 H. Q. Wu, B. B. Tang and P. Y. Wu, *J. Membr. Sci.*, 2010, **362**, 374–383.
37 L. Zhang, P. Xiao, W. Lu, J. W. Zhang, J. C. Gu, Y. J. Huang and T. Chen, *Adv. Mater. Interfaces*, 2016, **3**, 7.
38 L. Zhang, Y. Z. Tao, P. Xiao, L. W. Dai, L. P. Song, Y. J. Huang, J. W. Zhang, S. W. Kuo and T. Chen, *Adv. Mater. Interfaces*, 2017, **4**, 8.
39 B. Streszewski, W. Jaworski, K. Paclawski, E. Csapo, I. Dekany and K. Fitzner, *Colloids Surf., A*, 2012, **397**, 63–72.
40 T. Sharif, A. Niaz, M. Najeeb, M. I. Zaman, M. Ihsan and Sirajuddin, *Sens. Actuators, B*, 2015, **216**, 402–408.
41 J. Zhou, X. Zha, X. Zhou, F. Chen, G. Gao, S. Wang, C. Shen, T. Chen, C. Zhi, P. Eklund, S. Du, J. Xue, W. Shi, Z. Chai and Q. Huang, *ACS Nano*, 2017, **11**, 3841–3850.
42 J. Zhou, X. H. Zha, F. Y. Chen, Q. Ye, P. Eklund, S. Y. Du and Q. Huang, *Angew. Chem., Int. Ed.*, 2016, **55**, 5008–5013.
43 M. Dahlqvist, B. Alling and J. Rosen, *Phys. Rev. B*, 2010, **81**, 4.
44 Z. Q. Huang, D. Raciti, S. N. Yu, L. Zhang, L. Deng, J. He, Y. J. Liu, N. M. Khashab, C. Wang, J. L. Gong and Z. H. Nie, *J. Am. Chem. Soc.*, 2016, **138**, 6332–6335.